Supplement of Atmos. Chem. Phys., 24, 7961–7981, 2024
https://doi.org/10.5194/acp-24-7961-2024-supplement

Atmospheric Chemistry and Physics Open Access

Supplement of

Secondary reactions of aromatics-derived oxygenated organic molecules lead to plentiful highly oxygenated organic molecules within an intraday OH exposure

Yuwei Wang et al.

Correspondence to: Hefeng Zhang (zhanghf@craes.org.cn) and Lin Wang (lin_wang@fudan.edu.cn)

Text S1. Estimation of the OH reaction rate of $C_{18}H_{26}O_8$

The proposed structure of $C_{18}H_{26}O_8$ is shown in Figure S4 to help understanding but the potential cis-trans isomerism is not considered in this study.

A reaction rate constant for a OH-initiated reaction is defined in terms of a summation of partial rate constants for OH addition and H-atom abstraction by OH. There are two -CH=C< structure units in the $C_{18}H_{26}O_8$. The rate constant for OH addition to -CH=C< bond depends on the number, identity and position of substituent groups around it, of which the effects on the rate constants are quantitatively shown as substituent factors. For isolated C=C bonds in the alkenes, Peeters et al. defined site-specific parameters for addition of OH, i.e., $k_{pri\text{-}add}$, $k_{sec\text{-}add}$, and $k_{tert\text{-}add}$, respectively, to form primary, secondary and tertiary β-hydroxyalkyl radicals (Peeters et al., 2007). According to results of a previous study (Jenkin et al., 2018), $k_{sec\text{-}add}$, and $k_{tert\text{-}add}$ at 298 K are 2.63×10^{-11} cm^3 molecule^{-1} s^{-1} and 5.15×10^{-11} cm^3 molecule^{-1} s^{-1}, respectively. The -CH=C< structure units have two sites where OH can be attached to form a secondary and a tertiary β-hydroxyalkyl radical, respectively. One of the sites is neighboring to the >CH-O-O-CH< functional group and the other one to the bicyclic peroxide functional group. To our best knowledge, the activating effect on OH reactivity of the >CH-O-O-CH< functional group and bicyclic peroxide functional group was not previously reported. In a previous work, the activating effect of -OOH is suggested to be identical to -OH and -OOR (Jenkin et al., 2018). Therefore, the >CH-O-O-CH< peroxy linkage functional group and bicyclic peroxide functional group are assumed to have the same activating effects as -CH_2OOH, -CH(OOH), and -C(OOH)<, whose substituent factors for the addition OH to C=C bonds are 1.2. Hence, the OH addition reaction rate constant is estimated to be 9.34×10^{-11} cm^3 molecule^{-1} s^{-1}.

Abstraction of H atoms is typically much slower than OH addition. Previous studies also assumed that the abstraction of H atoms from the aromatic ring is negligible under atmospheric conditions based on reported data for the reaction of OH with benzene (Calvert et al., 2002). The rate coefficient for H-atom abstraction from OH group in phenol is around 2.6×10^{-12} cm^3 molecule^{-1} s^{-1} at 298 K (Atkinson et al., 1992; Coeur-Tourneur et al., 2006; Olariu et al., 2002; Berndt and Böge, 2003). This is already around a factor of 20 greater than estimated values for abstraction from -OH groups in aliphatic compounds, which is around 1.4×10^{-13} cm^3 molecule^{-1} s^{-1} at 298 K if no influences from neighboring substituent groups are considered (Jenkin et al., 2018; Kwok and Atkinson, 1995). Here, we only considered the H-atom abstraction on the -CH=C< structure units in $C_{18}H_{26}O_8$ as the H-atom abstraction on other positions is too slow. The group rate coefficient for H-atom abstraction from tertiary carbon is 1.49×10^{-12} cm^3 molecule^{-1} s^{-1} and the substituent factor related to H-atom abstraction reactions of OH adjacent to this double bond is 6.2. In addition, the empirical ring-strain factor has to be applied on the H-atom abstraction because of the C=C bond is in a 7-member ring structure, which is 1.12. Hence, the H-abstraction rate constant is calculated to be 1.03×10^{-11} cm^3 molecule^{-1} s^{-1}. No adjustments were made for potential impacts of ring strain effects on the OH addition rate constant as suggested by Jenkin et al.(2018).

As a final step, because there are two -CH=C< structure units in $C_{18}H_{26}O_8$, the total OH reaction rate constant needs to be multiplied by 2, which is 2.07×10^{-10} cm^3 molecule^{-1} s^{-1}.

The distribution of errors ($\log k_{calc}/k_{obs}$, where k_{calc} and k_{obs} are the calculated and observed OH reaction rate, respectively) for cyclic alkenes of the SAR methods updated by Jenkin et al. has a root mean squared error (RMSE) of 0.11 and a mean absolute error (MAE) of 0.082 (Jenkin et al., 2018),

corresponding to an uncertainty within $^{+28.8}_{-23.3}$% for the calculated OH reaction rate constants of $C_{18}H_{26}O_8$. Therefore, the total OH reaction rate constant of $C_{18}H_{26}O_8$ is in the range of 1.61 – 2.67 $\times 10^{-10}$ cm^3 $molecule^{-1}$ s^{-1}.

Table S1. Summary of experimental conditions.

No.	Initial concentration of 1,3,5-TMB ($\times10^{11}$ molecule cm^{-3})	O_3 concentration ($\times10^{12}$ molecule cm^{-3})*	NO concentration ($\times10^{10}$ molecule cm^{-3})	NO_2 concentration ($\times10^{11}$ molecule cm^{-3})	Estimated OH exposure based on the precursor consumption ($\times10^{9}$ molecule cm^{-3} s)
1-1	13.4	11.0	0	0	18.5
1-2	14.4	11.1	0	0	11.2
1-3	15.4	11.4	0	0	5.2
1-4	9.4	10.6	0	0	44.0
1-5	9.8	10.8	0	0	40.9
1-6	10.1	10.9	0	0	34.8
1-7	10.3	11.1	0	0	28.7
1-8	10.7	11.3	0	0	21.9
1-9	11.2	11.5	0	0	13.3
1-10	11.5	11.7	0	0	6.3
1-11	11.7	11.8	0	0	5.9
1-12	11.8	11.8	0	0	44.9
1-13	11.9	10.5	0	0	39.8
1-14	11.7	10.6	0	0	35.9
1-15	11.7	10.9	0	0	31.5
1-16	12.0	11.0	0	0	26.8
1-17	12.1	11.2	0	0	18.9
1-18	12.2	11.4	0	0	11.3
1-19	12.3	11.8	0	0	5.3
1-20	7.1	10.5	0	0	48.7
1-21	7.7	10.5	0	0	48.1
1-22	8.0	10.5	0	0	44.1
1-23	8.2	10.8	0	0	38.1
1-24	8.3	11.0	0	0	32.5
1-25	8.4	11.1	0	0	23.8
1-26	8.5	11.4	0	0	16.1
1-27	12.2	10.4	0	0	41.9
1-28	12.4	10.6	0	0	37.8
1-29	12.3	10.8	0	0	34.3
1-30	12.4	11.0	0	0	29.7
1-31	12.6	11.2	0	0	24.4
1-32	12.6	11.4	0	0	17.8
1-33	12.9	11.7	0	0	10.6
1-34	11.4	10.5	0	0	43.5
1-35	11.6	10.7	0	0	38.5
1-36	11.7	10.8	0	0	35.2
1-37	12.0	11.0	0	0	30.1

1-38	12.3	11.3	0	0	25.6
1-39	12.4	11.4	0	0	18.1
1-40	12.6	11.7	0	0	11.6
1-41	7.3	21.2	4.9	14.7	31.1
1-42	9.1	21.0	4.5	15.7	28.9
1-43	10.9	20.9	4.6	16.4	27.3
1-44	12.8	20.9	4.3	16.7	25.7
1-45	14.6	21.0	4.2	17.2	24.1
1-46	16.6	21.0	4.0	17.4	22.6
1-47	6.6	21.1	4.8	15.9	31.9
1-48	7.7	21.4	4.7	16.7	30.9
1-49	9.7	21.4	4.5	17.2	28.6
1-50	11.4	21.5	4.3	17.6	27.0
1-51	13.5	21.6	4.2	17.9	25.3
1-52	15.9	21.6	4.0	18.1	23.6
1-53	18.0	21.2	3.9	18.4	21.9
1-54	20.6	21.6	3.9	19.1	20.6
1-55	7.2	17.5	11.8	25.5	39.8
1-56	8.7	17.2	11.8	27.2	37.7
1-57	4.1	17.0	13.0	26.7	41.8
1-58	5.6	17.1	12.8	27.4	41.4
1-59	7.3	17.1	12.0	28.7	38.4
1-60	8.8	1.71	11.5	29.2	36.2
1-61	10.1	1.71	11.1	29.9	34.3
1-62	11.4	16.9	11.3	31.4	33.1
1-63	12.8	17.0	11.0	31.9	31.8
1-64	6.1	16.5	13.4	30.6	38.9
1-65	7.6	16.7	13.0	31.1	36.8
1-66	9.0	16.9	12.3	32.1	34.7
1-67	10.4	16.9	12.0	32.3	33.3
1-68	11.9	16.9	11.4	32.8	32.2
2-1	7.6	3.6	0	0	5.5
2-2	7.6	3.7	0	0	2.4
2-3	7.6	3.7	0	0	1.0
2-4	7.6	3.7	0	0	0.6
2-5	8.5	3.0	17.4	9.3	3.1
2-6	8.5	3.4	7.6	5.2	2.0
2-7	8.5	3.5	3.2	2.7	0.9

* O_3 concentrations were stable values measured after the lights were turned on.

Table S2. Reactions included in the modified PAM_chem_v8 model under the settings with only 254 nm UV lights on. For experiments in the absence of NO_x, the input value of N_2O is 0 and all the NO_x-related reactions actually proceed with a zero rate. RO_2 is the sum of BPR and $C_9H_{13}O_7$· for simplification.

No	Reactions	Reaction rate constants/photolysis rate (molecule^{-1} cm^3 s^{-1}/ s^{-1})
1	$HO_2 + h\nu$ (λ = 254 nm) = OH + O(^{1}D)	$2.63\times10^{-19}\times flux_{254}$
2	$O_3 + h\nu$ (λ = 254 nm) = OH + O(^{1}D)	$1.03\times10^{-17}\times flux_{254}$
3	H_2O + O(^{1}D) = 2OH	$1.63\times10^{-10}\times e^{60/T}$
4	N_2 + O(^{1}D) = O(^{3}P)	$2.15\times10^{-11}\times e^{110/T}$
5	O_2 + O(^{1}D) = O(^{3}P)	$3.30\times10^{-11}\times e^{55/T}$
6	O_3 + O(^{1}D) = 2O_2	1.20×10^{-10}
7	O_3 + O(^{1}D) = O + O + O_2	1.20×10^{-10}
8	O + OH = H + O_2	$2.20\times10^{-11}\times e^{120/T}$
9	O(^{1}D) + H_2 = OH + H	1.20×10^{-10}
10	HO_2 + H = 2OH	7.20×10^{-11}
11	HO_2 + H = O + H_2O	1.60×10^{-12}
12	HO_2 + H = H_2 + O_2	6.90×10^{-12}
13	O_3 + H = OH + O_2	$1.40\times10^{-11}\times e^{-470/T}$
14	N_2O + O(^{1}D) = 2NO	$6.70\times10^{-11}\times e^{20/T}$
15	N_2O + O(^{1}D) = N_2 + O_2	$4.70\times10^{-11}\times e^{20/T}$
16	O + HO_2 = OH + O_2	$3.02\times10^{-11}\times e^{200/T}$
17	O + H_2O_2 = OH + HO_2	$1.40\times10^{-12}\times e^{-2000/T}$
18	O + O_3 = 2O_2	$8.00\times10^{-12}\times e^{-2060/T}$
19	O + NO_3 = NO_2 + O_2	1.00×10^{-11}
20	O + NO_2 = NO + O_2	$5.12\times10^{-12}\times e^{210/T}$
21	OH + O_3 = HO_2 + O_2	$1.70\times10^{-12}\times e^{-940/T}$
22	OH + HO_2 = H_2O + O_2	$4.80\times10^{-11}\times e^{250/T}$
23	OH + HONO = H_2O + NO_2	$1.80\times10^{-11}\times e^{-390/T}$
24	OH + H_2O_2 = H_2O + HO_2	$2.90\times10^{-12}\times e^{-160/T}$
25	OH + H_2 = H_2O + H	$2.80\times10^{-12}\times e^{-1800/T}$
26	OH + OH = H_2O + O	1.80×10^{-12}
27	HO_2 + O_3 = OH + O_2	$1.00\times10^{-14}\times e^{-490/T}$
28	HO_2 + NO = OH + NO_2	$3.50\times10^{-12}\times e^{270/T}$
29	NO + O_3 = NO_2 + O_2	$2.00\times10^{-12}\times e^{-1400/T}$
30	NO_2 + O_3 = NO_3 + O_2	$1.20\times10^{-13}\times e^{-2450/T}$
31	NO + NO_3 = 2NO + O_2	$1.50\times10^{-11}\times e^{170/T}$
32	NO_3 + NO_3 = 2NO_2 + O_2	$8.50\times10^{-13}\times e^{-2450/T}$
33	N_2O_5 + H_2O = 2HNO_3	2.00×10^{-21}
34	O + O_2 + M = O_3 + M	$6.00\times10^{-34}\times M\times(300/T)^{2.4}$
35	H + O_2 + M = HO_2 + M	$k_o = 4.40\times10^{-32}\times M\times(300/T)^{1.3}$ $k_h = 7.50\times10^{-11}\times(300/T)^{0.2}$

		$k = k_o/(1+(k_o/k_h))\times 0.6^{(1+(\log10(k_o/k_h))^{-2}}$
36	$OH + OH + M = H_2O_2 + M$	$k_o = 6.90\times10^{-31}\times M\times(300/T)$ $k_h = 2.60\times10^{-11}$
		$k = k_o/(1+(k_o/k_h))\times 0.6^{(1+(\log10(k_o/k_h))^{-2}}$
37	$OH + NO + M = HONO + M$	$k_o = 7.00\times10^{-31}\times M\times(300/T)^{2.6}$ $k_h = 3.60\times10^{-11}\times(300/T)^{0.1}$
		$k = k_o/(1+(k_o/k_h))\times 0.6^{(1+(\log10(k_o/k_h))^{-2}}$
38	$OH + NO_2 + M = HNO_3 + M$	$k_o = 1.80\times10^{-30}\times M\times(300/T)^{2.6}$ $k_h = 2.80\times10^{-11}$
		$k = k_o/(1+(k_o/k_h))\times 0.6^{(1+(\log10(k_o/k_h))^{-2}}$
39	$OH + HNO_3 = H_2O + NO_3$	$k_{00} = 2.40\times10^{-14}\times e^{460/T}$ $k_{01} = 6.50\times10^{-34}\times e^{2199/T}$ $k_{02} = 2.80\times10^{-11}\times e^{-2450/T}$ $k = k_{00} + (k_{01}\times M)/(1+(k_{01}\times M)/k_{02})$
40	$HO_2 + NO_2 + M = HO_2NO_2 + M$	$k_o = 1.80\times10^{-31}\times M\times(300/T)^{3.2}$ $k_h = 4.70\times10^{-12}\times(300/T)^{1.4}$
		$k = k_o/(1+(k_o/k_h))\times 0.6^{(1+(\log10(k_o/k_h))^{-2}}$
41	$NO_2 + NO_3 + M = N_2O_5 + M$	$k_{reverse} = k/(2.10\times10^{-27}\times e^{10900/T})$ $k_o = 2.00\times10^{-30}\times M\times(300/T)^{4.4}$ $k_h = 1.40\times10^{-12}\times(300/T)^{0.7}$
		$k = k_o/(1+(k_o/k_h))\times 0.6^{(1+(\log10(k_o/k_h))^{-2}}$
		$k_{reverse} = k/(2.70\times10^{-27}\times e^{11000/T})$
42	$OH + HNO_4 =$ products	$1.30\times10^{-12}\times e^{250/T}$
43	$Sci + H_2O =$ products	4.00×10^{-15}
44	1,3,5-TMB + OH = BPR	$0.8\times5.67\times10^{-11}$
45	1,3,5-TMB + OH = Products	$0.2\times5.67\times10^{-11}$
46	BPR = C9H13O7	0.078
47	$BPR + RO_2 = ROOR'$	1.70×10^{-10}
48	$BPR + RO_2 = R{=}O/ROH + O_2$	$0.4\times8.8\times10^{-13}$
49	$BPR + RO_2 = 2RO + O_2$	$0.6\times8.8\times10^{-13}$
50	$BPR + OH = RPO_2 + H_2O$	1.00×10^{-10}
51	$BPR + HO_2 = ROOH + O_2$	1.50×10^{-11}
52	BPR = wall loss	0.0023
53	$BPR + NO = RO + NO_2$	$0.843\times8.50\times10^{-12}$
54	$BPR + NO + M = RONO_2 + M$	$0.157\times8.50\times10^{-12}$
55	$C_9H_{13}O_7 + RO_2 = ROOR'$	2.60×10^{-10}
56	$C_9H_{13}O_7 + RO_2 = R{=}O/ROH + O_2$	$0.4\times8.8\times10^{-13}$
57	$C_9H_{13}O_7 + RO_2 = 2RO + O_2$	$0.6\times8.8\times10^{-13}$

58	$C_9H_{13}O_7 + OH = RPO_2 + H_2O$	1.00×10^{-10}
59	$C_9H_{13}O_7 + HO_2 = ROOH + O_2$	1.50×10^{-11}
60	$C_9H_{13}O_7$ = wall loss	0.0023
61	$C_9H_{13}O_7$+ NO = RO + NO_2	$0.843\times8.50\times10^{-12}$
62	$C_9H_{13}O_7$ + NO + M = $RONO_2$+ M	$0.157\times8.50\times10^{-12}$
63	ROOH + OH = $RO_2 + H_2O$	$5.30\times10^{-12}\times e^{190/T}\times0.6$
64	ROOH + OH = RPHO + OH + H_2O	$5.30\times10^{-12}\times e^{190/T}\times0.4$
65	RO + O_2 = RPO + HO_2	6.00×10^{-15}
66	H_2O_2 + *hv* (λ = 254 nm) = 2OH	$6.70\times10^{-20}\times flux_{254}$
67	NO_2 + *hv* (λ = 254 nm) = O + NO	$1.00\times10^{-20}\times flux_{254}$
68	HONO + *hv* (λ = 254 nm) = OH + NO	$1.40\times10^{-19}\times flux_{254}$
69	HNO_3 + *hv* (λ = 254 nm) = OH + NO_2	$1.95\times10^{-20}\times flux_{254}$
70	HNO_4 + *hv* (λ = 254 nm) = HO_2 + NO_2	$3.60\times10^{-19}\times flux_{254}$
71	N_2O_5 + *hv* (λ = 254 nm) = NO_2 + NO_3	$3.20\times10^{-19}\times flux_{254}$

Table S3. The branching ratios of different pathways for $CH_3O_2\cdot$ + OH.

Reactions	Branching ratio	References
$CH_3O_2\cdot + OH \rightarrow CH_2O_2\cdot + H_2O$	< 5%	(Yan et al., 2016)
	0	(Caravan et al., 2018; Müller et al., 2016)
$CH_3O_2\cdot + OH \rightarrow CH_3O\cdot + HO_2$	86%	(Müller et al., 2016)
$CH_3O_2\cdot + OH \rightarrow CH_3OH + HO_2$	6 ± 2%	(Caravan et al., 2018)
	7%	(Müller et al., 2016)
$CH_3O_2\cdot + OH \rightarrow CH_3OOOH$	7%	(Müller et al., 2016)

Table S4. Summary of radical concentrations estimated by the PAM_chem_v8 model in the 2nd-round experiments.

	Estimated [OH] with PAM_chem_v8 based on the precursor consumption ($\times 10^7$ molecule cm^{-3})	Estimated [HO_2] with PAM_chem_v8 based on the precursor consumption ($\times 10^8$ molecule cm^{-3})	Estimated [RO_2] with PAM_chem_v8 based on the precursor consumption ($\times 10^9$ molecule cm^{-3})
2-1	10.3	3.73	4.05
2-2	4.54	2.14	2.80
2-3	1.64	0.97	1.69
2-4	1.04	0.67	1.34
2-5	5.80	13.1	1.55
2-6	3.69	11.5	1.39
2-7	1.69	8.38	1.07

Table S5. Molecular formulae and molar masses of observed HOM monomers and dimers in the high [OH], NO_x-free experiments, along with their relative contributions to the total HOMs signals when OH exposure equaled 2.38×10^{10} molecules cm^{-3} s (Exp. 1-25).

Molecular formula	Molar mass (Th)	Contributions to total HOMs signals (%)
$C_7H_8O_7$	204.0270	0.19
$C_8H_{12}O_6$	204.0634	0.20
$C_7H_{10}O_7$	206.0427	0.39
$C_9H_{12}O_6$	216.0634	0.40
$C_9H_{13}O_6$	217.0712	0.15
$C_8H_{10}O_7$	218.0427	1.22
$C_9H_{14}O_6$	218.0790	1.17
$C_8H_{11}O_7$	219.0505	0.24
$C_9H_{15}O_6$	219.0869	0.14
$C_7H_8O_8$	220.0219	0.14
$C_8H_{12}O_7$	220.0583	0.90
$C_9H_{16}O_6$	220.0947	0.68
$C_7H_{10}O_8$	222.0376	0.45
$C_8H_{14}O_7$	222.0740	0.22
$C_9H_{12}O_7$	232.0583	0.72
$C_9H_{13}O_7$	233.0661	0.24
$C_9H_{14}O_7$	234.0740	6.02
$C_9H_{15}O_7$	235.0818	2.35
$C_9H_{16}O_7$	236.0896	3.72
$C_9H_{12}O_8$	248.0532	0.75
$C_9H_{13}O_8$	249.0610	0.11
$C_9H_{14}O_8$	250.0689	2.30
$C_9H_{15}O_8$	251.0767	2.15
$C_9H_{16}O_8$	252.0845	4.08
$C_9H_{13}O_9$	265.0560	0.36
$C_9H_{14}O_9$	266.0638	1.34
$C_9H_{15}O_9$	267.0716	0.95
$C_9H_{16}O_9$	268.0794	2.44
$C_9H_{12}O_{10}$	280.0430	0.23
$C_9H_{14}O_{10}$	282.0587	0.54
$C_9H_{15}O_{10}$	283.0665	0.27
$C_9H_{16}O_{10}$	284.0743	0.39
$C_9H_{12}O_{11}$	296.0380	0.16
$C_{18}H_{26}O_8$	370.1628	0.38
$C_{18}H_{24}O_9$	384.1420	0.31
$C_{18}H_{26}O_9$	386.1577	0.37
$C_{17}H_{24}O_{10}$	388.1369	0.31
$C_{18}H_{24}O_{10}$	400.1369	0.80
$C_{18}H_{26}O_{10}$	402.1526	9.49

$C_{18}H_{28}O_{10}$	404.1682	4.62
$C_{18}H_{24}O_{11}$	416.1319	0.82
$C_{18}H_{26}O_{11}$	418.1475	2.99
$C_{18}H_{28}O_{11}$	420.1632	7.67
$C_{18}H_{24}O_{12}$	432.1268	0.86
$C_{18}H_{26}O_{12}$	434.1424	6.44
$C_{18}H_{28}O_{12}$	436.1581	9.17
$C_{18}H_{30}O_{12}$	438.1737	1.49
$C_{18}H_{24}O_{13}$	448.1217	0.67
$C_{18}H_{26}O_{13}$	450.1373	3.26
$C_{18}H_{28}O_{13}$	452.1530	6.49
$C_{18}H_{30}O_{13}$	454.1686	1.15
$C_{18}H_{24}O_{14}$	464.1166	0.53
$C_{18}H_{26}O_{14}$	466.1323	1.87
$C_{18}H_{28}O_{14}$	468.1479	3.16
$C_{18}H_{30}O_{14}$	470.1636	1.64
Total monomer		35.5
Total dimer		64.5

Table S6. The C9 and C18 products detected by nitrate CI-ToF in Exp. 2-3. The exact mass is the mass without an adduct of a reagent ion of NO_3^-. "--" stands for the signal of a compound was below the detection limit.

Molecular formula	Molar mass (Th)	Contributions to total C9 and C18 products in Exp. 2-3 (%)	Contributions to total C9 and C18 products in Exp. 2-4 (%)	DBE
$C_9H_{13}O_4$	247.0698	0.28	--	3.5
$C_9H_{14}O_4$	248.0776	0.34	--	3
$C_9H_{12}O_5$	262.0569	1.03	2.03	4
$C_9H_{13}O_5$	263.0647	0.36	--	3.5
$C_9H_{14}O_5$	264.0725	1.03	1.73	3
$C_9H_{12}O_6$	278.0518	1.60	2.45	4
$C_9H_{13}O_6$	279.0596	0.63	6.54	3.5
$C_9H_{14}O_6$	280.0674	4.64	2.11	3
$C_9H_{16}O_6$	282.0831	1.41	2.39	2
$C_9H_{10}O_7$	292.0310	1.17	2.40	5
$C_9H_{12}O_7$	294.0467	1.56	3.38	4
$C_9H_{13}O_7$	295.0545	2.34	6.74	3.5
$C_9H_{14}O_7$	296.0623	6.52	3.43	3
$C_9H_{15}O_7$	297.0701	4.15	1.73	2.5
$C_9H_{16}O_7$	298.0780	5.03	5.25	2
$C_9H_{12}O_8$	310.0416	3.20	3.31	4
$C_9H_{13}O_8$	311.0494	0.59	--	3.5
$C_9H_{14}O_8$	312.0572	3.39	4.42	3
$C_9H_{15}O_8$	313.0651	2.40	2.08	2.5
$C_9H_{16}O_8$	314.0729	7.31	8.70	2
$C_9H_{12}O_9$	326.0365	2.22	2.54	4
$C_9H_{13}O_9$	327.0443	1.30	1.52	3.5
$C_9H_{14}O_9$	328.0522	2.02	2.55	3
$C_9H_{15}O_9$	329.0600	0.78	--	2.5
$C_9H_{16}O_9$	330.0678	1.43	2.46	2
$C_9H_{12}O_{10}$	342.0314	1.61	1.83	4
$C_9H_{13}O_{10}$	343.0393	0.49	--	3.5
$C_9H_{14}O_{10}$	344.0471	1.07	--	3
$C_9H_{15}O_{10}$	345.0549	0.24	--	2.5
$C_9H_{16}O_{10}$	346.0627	0.37	--	2
$C_9H_{12}O_{11}$	358.0263	2.24	3.13	4
$C_9H_{13}O_{11}$	359.0342	0.60	--	3.5
$C_9H_{14}O_{11}$	360.0420	0.46	--	3
$C_9H_{15}O_{11}$	361.0498	0.19	--	2.5
$C_{18}H_{24}O_8$	430.1355	0.56	--	7
$C_{18}H_{26}O_8$	432.1511	4.83	5.86	6
$C_{18}H_{24}O_9$	446.1304	0.59	--	7
$C_{18}H_{26}O_9$	448.1461	1.35	2.53	6

$C_{18}H_{24}O_{10}$	462.1253	0.45	--	7
$C_{18}H_{25}O_{10}$	463.1332	0.36	--	6.5
$C_{18}H_{26}O_{10}$	464.1410	9.58	9.36	6
$C_{18}H_{28}O_{10}$	466.1566	2.97	2.42	5
$C_{18}H_{24}O_{11}$	478.1202	0.51	--	7
$C_{18}H_{26}O_{11}$	480.1359	2.28	2.15	6
$C_{18}H_{27}O_{11}$	481.1437	1.09	1.42	5.5
$C_{18}H_{28}O_{11}$	482.1515	2.44	1.70	5
$C_{18}H_{26}O_{12}$	496.1308	1.61	1.84	6
$C_{18}H_{28}O_{12}$	498.1465	1.13	--	5
$C_{18}H_{30}O_{12}$	500.1621	0.35	--	4
$C_{18}H_{24}O_{13}$	510.1101	0.33	--	7
$C_{18}H_{26}O_{13}$	512.1257	0.83	--	6
$C_{18}H_{27}O_{13}$	513.1335	0.51	--	5.5
$C_{18}H_{28}O_{13}$	514.1414	0.69	--	5
$C_{18}H_{30}O_{13}$	516.1570	0.33	--	4
$C_{18}H_{26}O_{14}$	528.1206	0.67	--	6
$C_{18}H_{27}O_{14}$	529.1284	0.17	--	5.5
$C_{18}H_{28}O_{14}$	530.1363	0.37	--	5
$C_{18}H_{30}O_{14}$	532.1519	0.30	--	4
$C_{18}H_{26}O_{15}$	544.1155	0.31	--	6
$C_{18}H_{27}O_{15}$	545.1234	0.24	--	5.5
$C_{18}H_{28}O_{15}$	546.1312	0.34	--	5
$C_{18}H_{30}O_{15}$	548.1469	0.21	--	4
$C_{18}H_{26}O_{16}$	560.1105	0.30	--	6
$C_{18}H_{28}O_{16}$	562.1261	0.30	--	5

Table S7. The C9 products detected by nitrate CI-ToF in Exp. 2-7.

Molecular formula	Molar mass (Th)	Contributions to total C9 and C18 products signals (%)	DBE
$C_9H_{12}O_6$	216.0634	1.25	4
$C_9H_{13}O_6$	217.0712	1.98	3.5
$C_9H_{14}O_6$	218.0790	1.95	3
$C_9H_{13}NO_6$	231.0743	3.97	3
$C_9H_{12}O_7$	232.0583	1.59	4
$C_9H_{13}O_7$	233.0661	2.92	3.5
$C_9H_{15}O_7$	235.0818	0.97	2.5
$C_9H_{13}NO_7$	247.0692	9.32	3
$C_9H_{12}O_8$	248.0532	3.11	4
$C_9H_{13}O_8$	249.0610	0.94	3.5
$C_9H_{14}O_8$	250.0689	2.15	3
$C_9H_{13}NO_8$	263.0641	21.25	3
$C_9H_{13}O_9$	265.0559	1.57	3.5
$C_9H_{15}NO_8$	265.0798	2.94	2
$C_9H_{13}NO_9$	279.0590	5.45	3
$C_9H_{12}O_{10}$	280.0430	1.91	4
$C_9H_{14}NO_9$	280.0669	3.34	2.5
$C_9H_{13}O_{10}$	281.0509	1.52	3.5
$C_9H_{15}NO_9$	281.0747	2.51	2
$C_9H_{14}N_2O_9$	294.0699	1.76	2
$C_9H_{13}NO_{10}$	295.0539	3.52	3
$C_9H_{14}N_2O_{10}$	310.0649	18.15	2
$C_9H_{13}NO_{11}$	311.0489	3.11	3
$C_9H_{12}N_2O_{11}$	324.0441	1.23	3
$C_9H_{14}N_2O_{11}$	326.0598	1.60	2

(a)

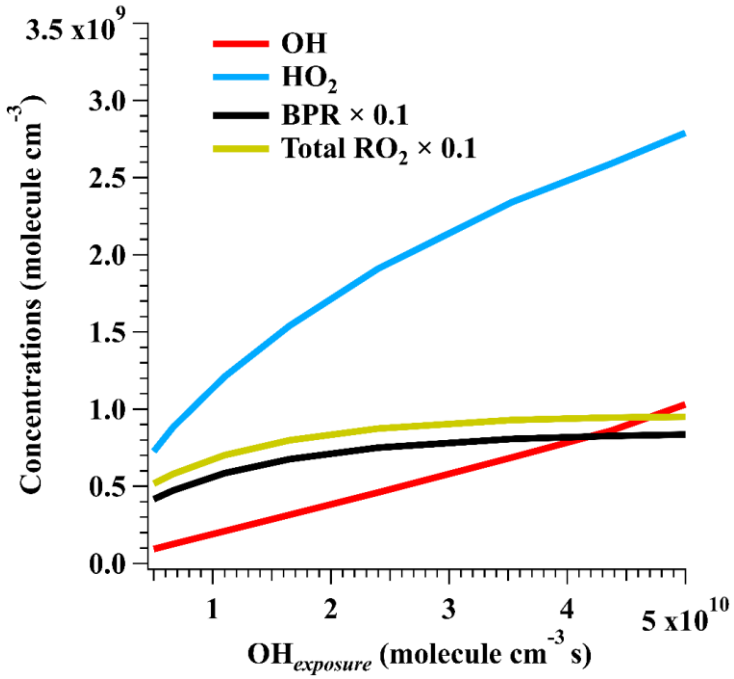

(b)

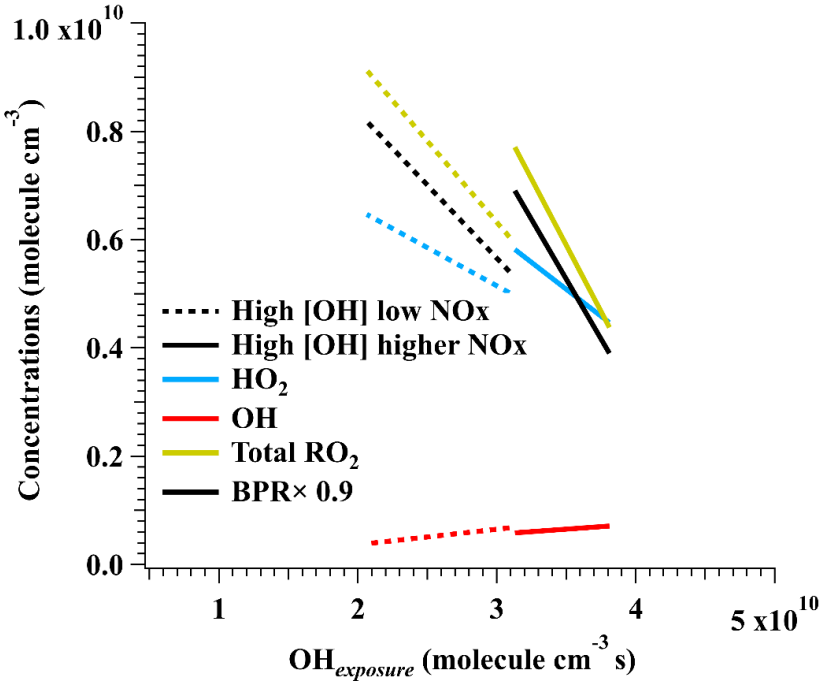

Figure S1. (a) Concentration profiles of OH, HO_2, BPR, and total RO_2 in the 1st-round experiments in the absent of NO_x in the PAM OFR as a function of OH exposures. The average total concentrations of RO_2 and BPR were scaled with a factor of 0.1 for a better visualization. (b) Concentration profiles of OH, HO_2, BPR, and total RO_2 in the 1st-round experiments in the presence of NO_x in the PAM OFR as a function of OH exposures. The average total concentrations of RO_2 were scaled with a factor of 0.9 for a better visualization.

(a)

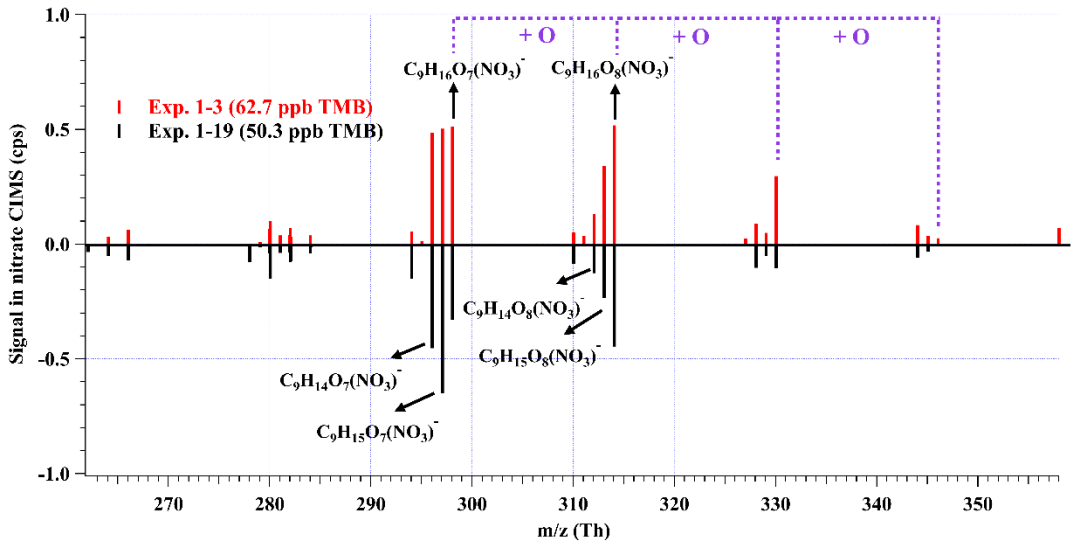
+ O
+ O
+ O
$C_9H_{16}O_7(NO_3)^-$
$C_9H_{16}O_8(NO_3)^-$
Exp. 1-3 (62.7 ppb TMB)
Exp. 1-19 (50.3 ppb TMB)
$C_9H_{14}O_8(NO_3)^-$
$C_9H_{15}O_8(NO_3)^-$
$C_9H_{14}O_7(NO_3)^-$
$C_9H_{15}O_7(NO_3)^-$
Signal in nitrate CIMS (cps)
m/z (Th)

(b)

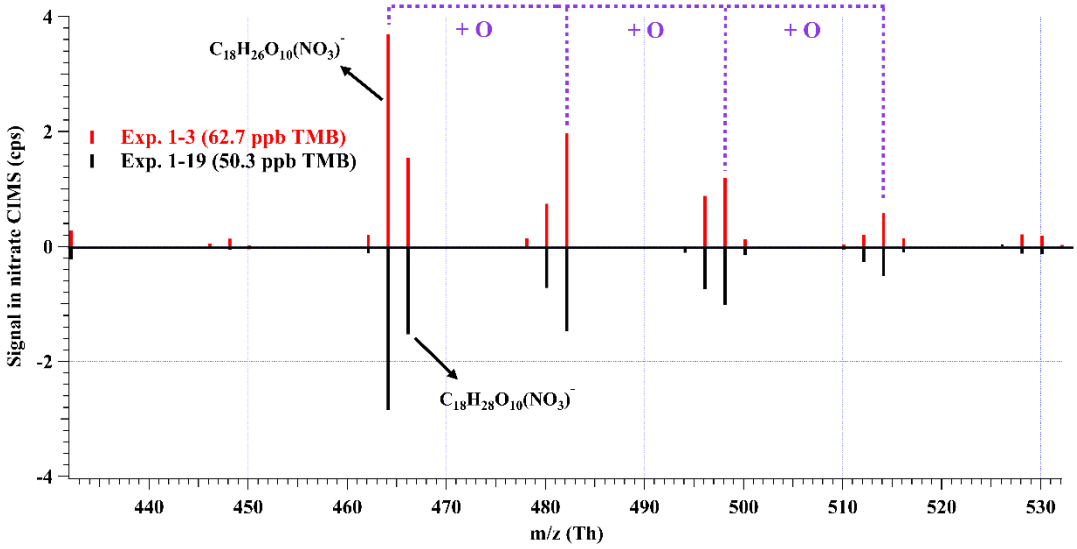
+ O
+ O
+ O
$C_{18}H_{26}O_{10}(NO_3)^-$
Exp. 1-3 (62.7 ppb TMB)
Exp. 1-19 (50.3 ppb TMB)
$C_{18}H_{28}O_{10}(NO_3)^-$
Signal in nitrate CIMS (cps)
m/z (Th)

(c)

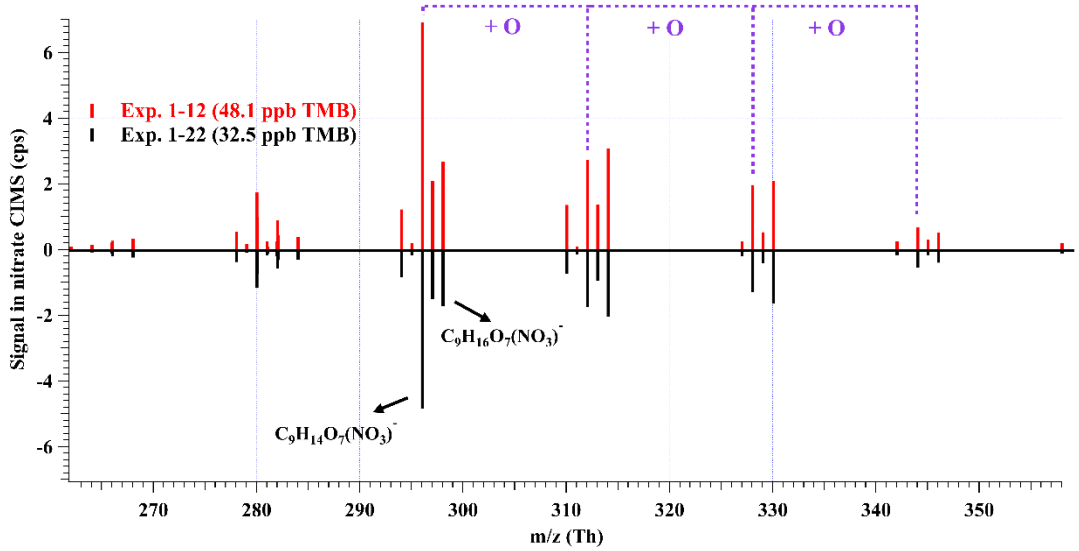

(d)

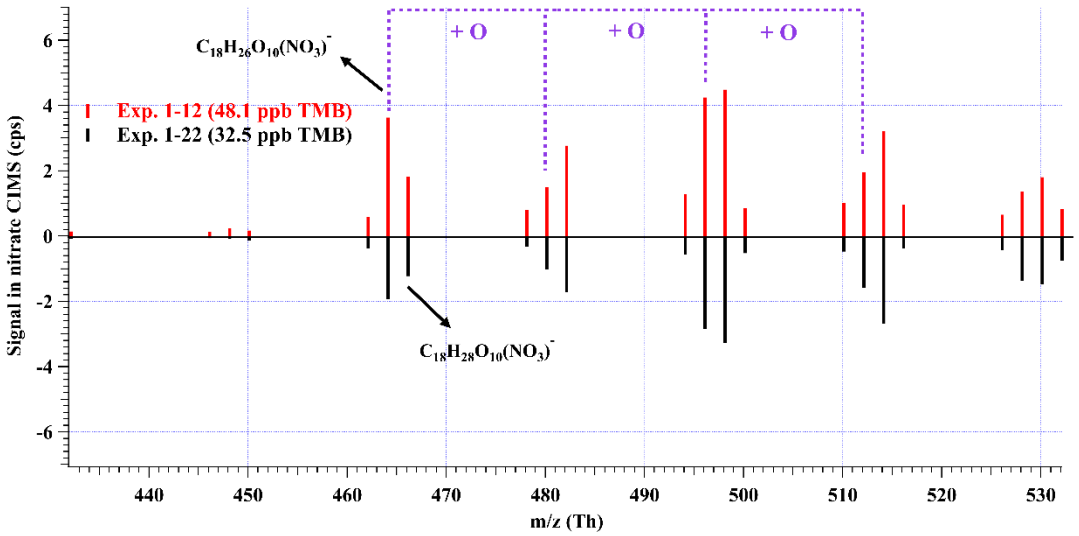

Figure S2. Mass spectra comparison of the (a) monomer products between Exp. 1-3 and Exp. 1-19, (b) dimer products between Exp. 1-3 and Exp. 1-19, (c) monomer product mass spectra between Exp. 1-12 and Exp. 1-22, and (d) dimer products between Exp. 1-12 and Exp. 1-22. The signals of HOMs were raw ones in the nitrate CIMS.

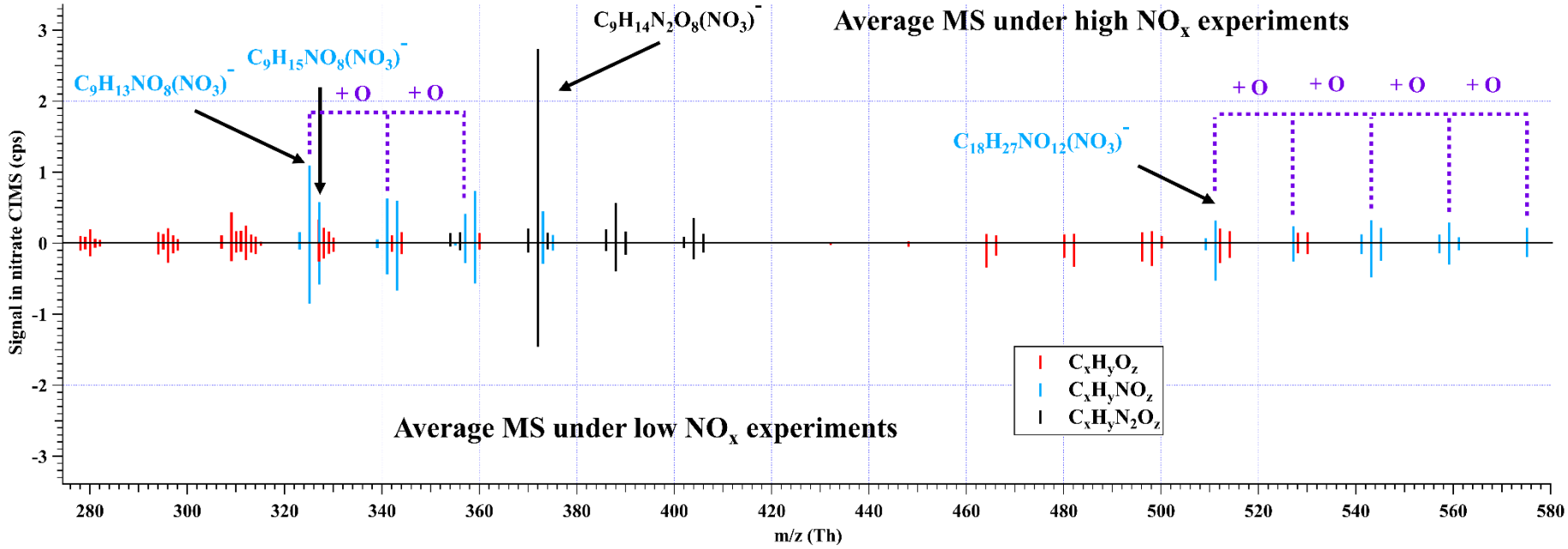

Figure S3. Average mass spectra of HOMs detected by nitrate CIMS in the 1st-round experiments with NO_x, presented with the averaged normalized signals in 4.41×10^{10} molecule cm^{-3} NO + 1.72×10^{12} molecule cm^{-3} NO_2 and 1.18×10^{11} molecule cm^{-3} NO + 2.94×10^{12} molecule cm^{-3} NO_2 experiments. For comparison, the mass spectra under the low NO_x experiments is shown in opposite values.

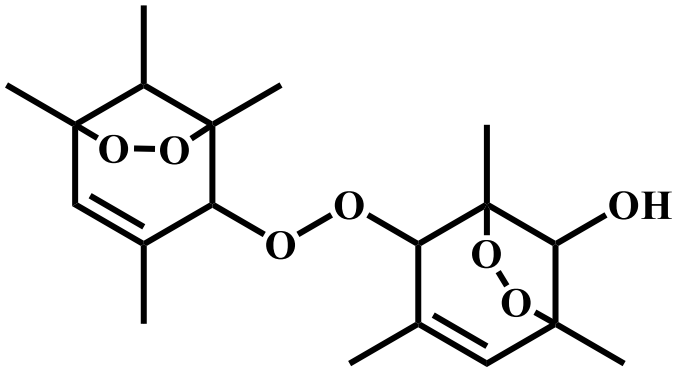

Figure S4. A plausible structure of $C_{18}H_{26}O_8$. The potential cis-trans isomerism is not shown.

References

Assaf, E., Song, B., Tomas, A., Schoemaecker, C., and Fittschen, C.: Rate Constant of the Reaction between CH 3 O 2 Radicals and OH Radicals Revisited , J. Phys. Chem. A, 120, 8923–8932, https://doi.org/10.1021/acs.jpca.6b07704, 2016.

Assaf, E., Tanaka, S., Kajii, Y., Schoemaecker, C., and Fittschen, C.: Rate constants of the reaction of C2–C4 peroxy radicals with OH radicals, Chem. Phys. Lett., 684, 245–249, https://doi.org/10.1016/j.cplett.2017.06.062, 2017.

Atkinson, R., Aschmann, S. M., and Arey, J.: Reactions of hydroxyl and nitrogen trioxide radicals with phenol, cresols, and 2-nitrophenol at 296 +- 2 K, Environ. Sci. Technol., 26, 1397–1403, https://doi.org/10.1021/es00031a018, 1992.

Berndt, T. and Böge, O.: Gas-phase reaction of OH radicals with phenol, Phys. Chem. Chem. Phys., 5, 342–350, https://doi.org/10.1039/b208187c, 2003.

Berndt, T., Scholz, W., Mentler, B., Fischer, L., Herrmann, H., Kulmala, M., and Hansel, A.: Accretion Product Formation from Self- and Cross-Reactions of RO2 Radicals in the Atmosphere, Angew. Chemie - Int. Ed., 57, 3820–3824, https://doi.org/10.1002/anie.201710989, 2018.

Bianchi, F., Kurtén, T., Riva, M., Mohr, C., Rissanen, M. P., Roldin, P., Berndt, T., Crounse, J. D., Wennberg, P. O., Mentel, T. F., Wildt, J., Junninen, H., Jokinen, T., Kulmala, M., Worsnop, D. R., Thornton, J. A., Donahue, N., Kjaergaard, H. G., and Ehn, M.: Highly Oxygenated Organic Molecules (HOM) from Gas-Phase Autoxidation Involving Peroxy Radicals: A Key Contributor to Atmospheric Aerosol, Chem. Rev., 119, 3472–3509, https://doi.org/10.1021/acs.chemrev.8b00395, 2019.

Bossolasco, A., Faragó, E. P., Schoemaecker, C., and Fittschen, C.: Rate constant of the reaction between CH3O2 and OH radicals, Chem. Phys. Lett., 593, 7–13, https://doi.org/10.1016/j.cplett.2013.12.052, 2014.

Brune, W. H.: The Chamber Wall Index for Gas-Wall Interactions in Atmospheric Environmental Enclosures, Environ. Sci. Technol., 53, 3645–3652, https://doi.org/10.1021/acs.est.8b06260, 2019.

Calvert, J. G., Becker, K. H., Kamens, R., Seinfeld, J., Wallington, T. J., and Yarwood, G.: The Mechanisms of Atmospheric Oxidation of the Aromatic Hydrocarbons, 2002.

Caravan, R. L., Khan, M. A. H., Zádor, J., Sheps, L., Antonov, I. O., Rotavera, B., Ramasesha, K., Au, K., Chen, M. W., Rösch, D., Osborn, D. L., Fittschen, C., Schoemaecker, C., Duncianu, M., Grira, A., Dusanter, S., Tomas, A., Percival, C. J., Shallcross, D. E., and Taatjes, C. A.: The reaction of hydroxyl and methylperoxy radicals is not a major source of atmospheric methanol, Nat. Commun., 9, 1–9, https://doi.org/10.1038/s41467-018-06716-x, 2018.

Cheng, X., Chen, Q., Li, Y. J., Zheng, Y., Liao, K., and Huang, G.: Highly Oxygenated Organic Molecules Produced by the Oxidation of Benzene and Toluene in a Wide Range of OH Exposure and NOx Conditions, Atmos. Chem. Phys., 1–23, https://doi.org/10.5194/acp-2021-201, 2021.

Coeur-Tourneur, C., Henry, F., Janquin, M. A., and Brutier, L.: Gas-phase reaction of hydroxyl radicals with m-, o- and p-cresol, Int. J. Chem. Kinet., 38, 553–562, https://doi.org/10.1002/kin.20186, 2006.

Crounse, J. D., Nielsen, L. B., Jørgensen, S., Kjaergaard, H. G., and Wennberg, P. O.: Autoxidation of organic compounds in the atmosphere, J. Phys. Chem. Lett., 4, 3513–3520, https://doi.org/10.1021/jz4019207, 2013.

Fittschen, C.: The reaction of peroxy radicals with OH radicals, Chem. Phys. Lett., 725, 102–108, https://doi.org/10.1016/j.cplett.2019.04.002, 2019.

Fuller, E. N., Schettler, P. D., and Giddings, J. C.: A new method for prediction of binary gas-phase diffusion coefficients, Ind. Eng. Chem., 58, 18–27, https://doi.org/10.1021/ie50677a007, 1966.

Jenkin, M. E., Saunders, S. M., Wagner, V., and Pilling, M. J.: Protocol for the development of the Master Chemical Mechanism, MCM v3 (Part B): tropospheric degradation of aromatic volatile organic compounds, Atmos. Chem. Phys., 3, 181–193, https://doi.org/10.5194/acp-3-181-2003, 2003.

Jenkin, M. E., Valorso, R., Aumont, B., Rickard, A. R., and Wallington, T. J.: Estimation of rate coefficients and branching ratios for gas-phase reactions of OH with aliphatic organic compounds for use in automated mechanism construction, 9297–9328 pp., https://doi.org/10.5194/acp-18-9297-2018, 2018.

Knap, H. C. and Jørgensen, S.: Rapid Hydrogen Shift Reactions in Acyl Peroxy Radicals, J. Phys. Chem. A, 121, 1470–1479, https://doi.org/10.1021/acs.jpca.6b12787, 2017.

Kwok, E. S. C. and Atkinson, R.: Estimation of hydroxyl radical reaction rate constants for gas-phase organic compounds using a structure-reactivity relationship: An update, Atmos. Environ., 29, 1685–1695, https://doi.org/10.1016/1352-2310(95)00069-B, 1995.

McMurry, P. H. and Grosjean, D.: Gas and Aerosol Wall Losses in Teflon Film Smog Chambers, Environ. Sci. Technol., 19, 1176–1182, https://doi.org/10.1021/es00142a006, 1985.

Molteni, U., Bianchi, F., Klein, F., Haddad, I. El, Frege, C., Rossi, M. J., Dommen, J., and Baltensperger, U.: Formation of highly oxygenated organic molecules from aromatic compounds, Atmos. Chem. Phys, 18, 1909–1921, https://doi.org/10.5194/acp-18-1909-2018, 2018.

Müller, J. F., Liu, Z., Nguyen, V. S., Stavrakou, T., Harvey, J. N., and Peeters, J.: The reaction of methyl peroxy and hydroxyl radicals as a major source of atmospheric methanol, Nat. Commun., 7, 1–11, https://doi.org/10.1038/ncomms13213, 2016.

Olariu, R. I., Klotz, B., Barnes, I., Becker, K. H., and Mocanu, R.: FT-IR study of the ring-retaining products from the reaction of OH radicals with phenol, o-, m-, and p-cresol, Atmos. Environ., 36, 3685–3697, https://doi.org/10.1016/S1352-2310(02)00202-9, 2002.

Palm, B. B., Campuzano-Jost, P., Ortega, A. M., Day, D. A., Kaser, L., Jud, W., Karl, T., Hansel, A., Hunter, J. F., Cross, E. S., Kroll, J. H., Peng, Z., Brune, W. H., and Jimenez, J. L.: In situ secondary organic aerosol formation from ambient pine forest air using an oxidation flow reactor, Atmos. Chem. Phys., 16, 2943–2970, https://doi.org/10.5194/acp-16-2943-2016, 2016.

Peeters, J., Boullart, W., Pultau, V., Vandenberk, S., and Vereecken, L.: Structure-activity relationship for the addition of OH to (poly)alkenes: Site-specific and total rate constants, J. Phys. Chem. A, 111, 1618–1631, https://doi.org/10.1021/jp066973o, 2007.

Peng, Z. and Jimenez, J. L.: Radical chemistry in oxidation flow reactors for atmospheric chemistry research, Chem. Soc. Rev., 49, 2570–2616, https://doi.org/10.1039/c9cs00766k, 2020.

Praske, E., Otkjær, R. V., Crounse, J. D., Hethcox, J. C., Stoltz, B. M., Kjaergaard, H. G., and Wennberg, P. O.: Atmospheric autoxidation is increasingly important in urban and suburban North America, Proc. Natl. Acad. Sci. U. S. A., 115, 64–69, https://doi.org/10.1073/pnas.1715540115, 2018.

Slater, E. J., Whalley, L. K., Woodward-Massey, R., Ye, C., Lee, J. D., Squires, F., Hopkins, J. R., Dunmore, R. E., Shaw, M., Hamilton, J. F., Lewis, A. C., Crilley, L. R., Kramer, L., Bloss, W., Vu, T., Sun, Y., Xu, W., Yue, S., Ren, L., Acton, W. J. F., Hewitt, C. N., Wang, X., Fu, P., and Heard, D. E.: Elevated levels of OH observed in haze events during wintertime in central Beijing, Atmos. Chem. Phys., 20, 14847–14871, https://doi.org/10.5194/acp-20-14847-2020, 2020.

Tan, Z., Rohrer, F., Lu, K., Ma, X., Bohn, B., Broch, S., Dong, H., Fuchs, H., Gkatzelis, G. I., Hofzumahaus, A., Holland, F., Li, X., Liu, Y., Liu, Y., Novelli, A., Shao, M., Wang, H., Wu, Y., Zeng, L., Hu, M., Kiendler-Scharr, A., Wahner, A., and Zhang, Y.: Wintertime photochemistry in Beijing: Observations of ROx radical concentrations in the North China Plain during the BEST-ONE campaign,

Atmos. Chem. Phys., https://doi.org/10.5194/acp-18-12391-2018, 2018.

Tsiligiannis, E., Hammes, J., Salvador, C. M., Mentel, T. F., and Hallquist, M.: Effect of NOx on 1,3,5-trimethylbenzene (TMB) oxidation product distribution and particle formation, Atmos. Chem. Phys., 19, 15073–15086, https://doi.org/10.5194/acp-19-15073-2019, 2019.

Wang, L., Wu, R., and Xu, C.: Atmospheric oxidation mechanism of benzene. Fates of alkoxy radical intermediates and revised mechanism, J. Phys. Chem. A, 117, 14163–14168, https://doi.org/10.1021/jp4101762, 2013.

Wang, S., Wu, R., Berndt, T., Ehn, M., and Wang, L.: Formation of Highly Oxidized Radicals and Multifunctional Products from the Atmospheric Oxidation of Alkylbenzenes, Environ. Sci. Technol., 51, 8442–8449, https://doi.org/10.1021/acs.est.7b02374, 2017.

Xu, L., Møller, K. H., Crounse, J. D., Kjaergaard, H. G., and Wennberg, P. O.: New insights into the radical chemistry and product distribution in the OH-initiated oxidation of benzene, Environ. Sci. Technol., 54, 13467–13477, https://doi.org/10.1021/acs.est.0c04780, 2020.

Yan, C., Kocevska, S., and Krasnoperov, L. N.: Kinetics of the Reaction of CH3O2 Radicals with OH Studied over the 292-526 K Temperature Range, J. Phys. Chem. A, 120, 6111–6121, https://doi.org/10.1021/acs.jpca.6b04213, 2016.